

# Redox-Switchable Direction of Photoinduced Electron Transfer in an $\text{Ru}(\text{bpy})_3^{2+}$ – Viologen Dyad\*\*

Reiner Lomoth,<sup>[a]</sup> Tilmann Häupl,<sup>[a]</sup> Olof Johansson,<sup>[b]</sup> and Leif Hammarström\*<sup>[a]</sup>

**Abstract:** Quenching of the  $^3\text{MLCT}$  excited state of  $[\text{Ru}(\text{bpy})_3]^{2+}$  (bpy = bipyridine) by the reduction products ( $\text{MV}^{•+}$  and  $\text{MV}^0$ ) of methyl viologen ( $\text{MV}^{2+}$ ) was studied by a combination of electrochemistry with laser flash photolysis or femtosecond pump–probe spectroscopy. Both for the bimolecular reactions and for the reactions in an  $\text{Ru}(\text{bpy})_3^{2+}$ – $\text{MV}^{n+}$  dyad, quenching by  $\text{MV}^{•+}$  and  $\text{MV}^0$  is reductive and gives the reduced ruthenium complex  $[\text{Ru}(\text{bpy})_3]^+$ , in contrast to the oxidative

quenching by  $\text{MV}^{2+}$ . Rate constants of quenching ( $k_q$ ), and thermal charge recombination ( $k_{\text{rec}}$ ) and cage escape yields ( $\phi_{\text{ce}}$ ) were determined for the bimolecular reactions, and rates of forward ( $k_f$ ) and backward ( $k_b$ ) electron transfer in the dyad were measured for quenching by  $\text{MV}^{2+}$ ,  $\text{MV}^{•+}$ , and  $\text{MV}^0$ .

**Keywords:** electrochemistry • electron transfer • molecular devices • ruthenium • viologens

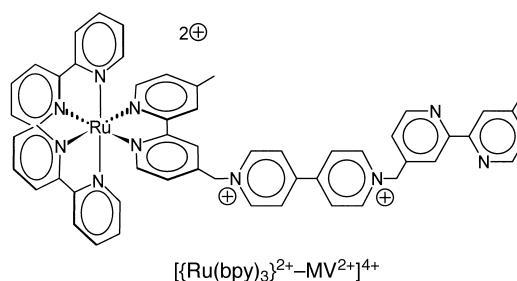
The reactions in the dyad are very rapid, with values up to  $k_f = 1.3 \times 10^{12} \text{ s}^{-1}$  for  $^*\text{Ru}(\text{bpy})_3^{2+}$ – $\text{MV}^{•+}$ . In addition, a long-lived ( $\tau = 15 \text{ ps}$ ) vibrationally excited state of  $\text{MV}^{•+}$  with a characteristically structured absorption spectrum was detected; this was generated by direct excitation of the  $\text{MV}^{•+}$  moiety both at 460 and 600 nm. The results show that the direction of photoinduced electron transfer in a  $\text{Ru}(\text{bpy})_3$ – $\text{MV}$  molecule can be switched by an externally applied bias.

## Introduction

The reaction of the  $^3\text{MLCT}$  excited state of  $[\text{Ru}(\text{bpy})_3]^{2+}$  (bpy = 2,2'-bipyridine) and methyl viologen ( $N,N'$ -dimethyl-4,4'-bipyridinium dication,  $\text{MV}^{2+}$ ) is a paradigm of oxidative electron-transfer quenching of transition metal complexes.<sup>[1]</sup> However, little is known about the reaction between  $^*[\text{Ru}(\text{bpy})_3]^{2+}$  and the reduction products of  $\text{MV}^{2+}$ : the radical cation ( $\text{MV}^{•+}$ ) and neutral methyl viologen ( $\text{MV}^0$ ).<sup>[2]</sup> The quenching mechanism can be expected to change from oxidative to reductive upon reduction of  $\text{MV}^{2+}$  to  $\text{MV}^{•+}$  (or  $\text{MV}^0$ ), since oxidative quenching by  $\text{MV}^{•+}$  would have a low driving force ( $\Delta G^0 \approx 0 \text{ eV}$ ). Due to the expected mechanistic change, the direction of photoinduced electron transfer in supramolecular  $\text{Ru}(\text{bpy})_3$ – $\text{MV}$  systems might be switched by an external potential bias or by sequential multiple excitation. An alternating role of a single molecular unit as both electron donor and acceptor allows the function of a molecular array to be switched, for use in molecular electronic devices.<sup>[3]</sup>

Wasielowski et al.<sup>[4]</sup> explored this type of concept by using sequential two-photon excitation, in which imides and diimides play the multifunctional role by being donors in the ground state and acceptors in the excited state, or vice versa. To the best of our knowledge, however, viologen derivatives have not been investigated for this purpose, and the reduced forms have not been used as reactants for excited state electron-transfer reactions.

We have applied a combination of electrochemistry with laser flash photolysis or femtosecond pump–probe spectroscopy to study the quenching of the excited state of  $[\text{Ru}(\text{bpy})_3]^{2+}$  by  $\text{MV}^{•+}$  or  $\text{MV}^0$  in a bimolecular reaction and as an intramolecular reaction in a  $\text{Ru}(\text{bpy})_3$ – $\text{MV}$  dyad. Thus,



we could verify the expected change in electron-transfer direction as the viologen is reduced prior to excitation. The  $\text{Ru}(\text{bpy})_3$ – $\text{MV}$  dyad behaves as a redox-switchable molecular photodiode, in which the photodiode response (electron-

[a] Dr. L. Hammarström, Dr. R. Lomoth, Dr. T. Häupl  
Department of Physical Chemistry, Uppsala University  
PO Box 532, 751 21 Uppsala (Sweden)  
Fax: (+46) 18-508542  
E-mail: leifh@fki.uu.se

[b] O. Johansson  
Department of Organic Chemistry, Arrhenius Laboratory  
Stockholm University, 106 91 Stockholm (Sweden)

[\*\*] bpy = bipyridine.

transfer direction) is controlled by an externally applied electronic bias. We report and discuss the kinetics of the different reaction steps in both the bimolecular system and the dyad, and provide data on the excited state dynamics of both the  $[\text{Ru}(\text{bpy})_3]^{2+}$  and  $\text{MV}^{2+}$  units. The rapidity of the reactions in the dyad, down to the subpicosecond timescale, demonstrates the potential of the system as a basis for a molecular switch.

## Results and Discussion

**Electrochemistry:** Cyclic voltammograms of  $\text{Ru}(\text{bpy})_3^{2+}$ – $\text{MV}^{2+}$  in acetonitrile show one quasireversible ( $\Delta E_p = 79$  mV) oxidation wave ( $E_{pa} = 0.92$  V vs  $\text{Fc}^+/\text{Fc}$ ) and five quasireversible ( $\Delta E_p = 60$ – $80$  mV) reduction waves ( $E_{pc}(1) = -0.71$ ,  $E_{pc}(2) = -1.11$ ,  $E_{pc}(3) = -1.77$ ,  $E_{pc}(4) = -1.97$ ,  $E_{pc}(5) = -2.24$  V). Differential pulse voltammograms show six well-resolved peaks of equal shape and height, each equivalent to a one-electron transfer. By comparison with the voltammograms observed for the model compounds  $[\text{Ru}(\text{bpy})_3]^{2+}$  and  $\text{MV}^{2+}$  under the same conditions, the voltammetric waves can be assigned to metal-centered oxidation ( $\text{Ru}^{\text{II}} \rightarrow \text{Ru}^{\text{III}}$ ) and two subsequent reductions of  $\text{MV}^{2+}$ , followed by reductions of the bpy ligands in the  $[\text{Ru}(\text{bpy})_3]$  moiety.<sup>[5]</sup> The data for the redox processes in  $\text{Ru}(\text{bpy})_3^{2+}$ – $\text{MV}^{2+}$  are compiled in Table 1 together with the corresponding data for  $[\text{Ru}(\text{bpy})_3]^{2+}$  and  $\text{MV}^{2+}$ . While the redox potentials for oxidation and reduction of  $[\text{Ru}(\text{bpy})_3]^{2+}$  and the corresponding processes in the dyad are basically identical, the reductions of the MV moiety in  $\text{Ru}(\text{bpy})_3^{2+}$ – $\text{MV}^{2+}$  are shifted to less cathodic potentials relative to free  $\text{MV}^{2+}$ . The shift of 155 mV for  $\text{MV}^{2+} \rightarrow \text{MV}^{+}$  and 150 mV for  $\text{MV}^{+} \rightarrow \text{MV}^0$  can be explained only partly by the effect of the  $[\text{Ru}(\text{bpy})_3]^{2+}$  moiety in  $\text{Ru}(\text{bpy})_3^{2+}$ – $\text{MV}^{2+}$ . This can account for 40–80 mV of the observed shift according to the results of Yonemoto et al.<sup>[6]</sup> The additional potential shift can be attributed to the electron-withdrawing effect of the bpy ligand, similar to the results reported for a *N*-cyanomethyl-substituted  $\text{Ru}(\text{bpy})_3$ –MV dyad.<sup>[6]</sup>

**Spectroelectrochemistry:** Spectroelectrochemical measurements on  $[\text{Ru}(\text{bpy})_3]^{2+}$ ,  $\text{MV}^{2+}$ , and  $\text{Ru}(\text{bpy})_3^{2+}$ – $\text{MV}^{2+}$  were performed to obtain accurate reference spectra of the reduced and oxidized compounds under the conditions employed for the time-resolved measurements and to check the stability of the dyad with the reduced methyl viologen moiety. By exhaustive electrolysis in an OTTLE-type (OTTLE = optically transparent thin-layer electrode) spectroelectrochemical cell at  $-1.03$  and  $-1.48$  V the characteristic electronic

absorption spectra of  $\text{MV}^{+}$  and  $\text{MV}^0$ , respectively, were observed. They are shown in Figure 1 together with the absorption spectrum of  $\text{MV}^{2+}$ . The spectra observed in acetonitrile containing  $0.1\text{ M } [\text{N}(\text{nC}_4\text{H}_9)_4]\text{PF}_6$  are in agreement

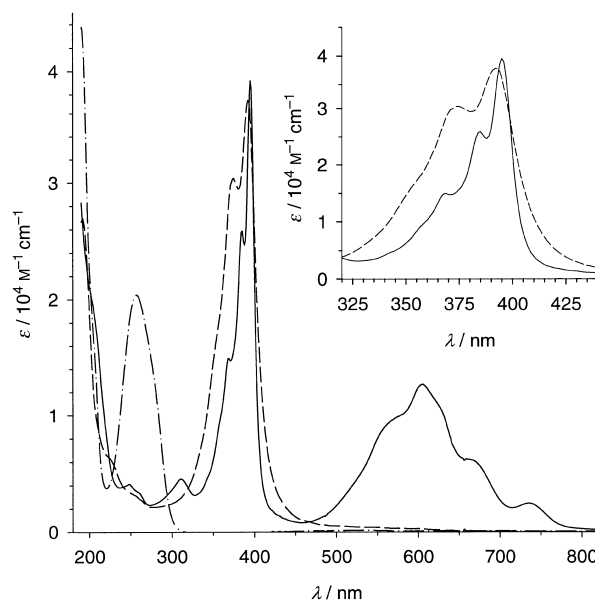


Figure 1. Spectroelectrochemical absorption spectra of  $\text{MV}^{2+}$  (—),  $\text{MV}^{+}$  (---), and  $\text{MV}^0$  (—•—) obtained by reduction of  $\text{MV}(\text{PF}_6)_2$  ( $0.53\text{ mM}$  in  $\text{CH}_3\text{CN}$ ,  $0.1\text{ M } [\text{N}(\text{nC}_4\text{H}_9)_4]\text{PF}_6$ ) at  $-1.03$  and  $-1.48$  V vs  $\text{Fc}^+/\text{Fc}$ . Inset: Details of the 400 nm bands of  $\text{MV}^{+}$  (—) and  $\text{MV}^0$  (—•—).

with those of the chloride salt,<sup>[7]</sup> and in particular no spectral signature attributable to the dimer  $(\text{MV}^{+})_2$ <sup>[8]</sup> was observed at the concentration of  $0.53\text{ mM}$  employed for the spectra shown in Figure 1. Extinction coefficients in Figure 1 are based on  $\epsilon_{260} = 20400\text{ M}^{-1}\text{ cm}^{-1}$  for  $\text{MV}^{2+}$ .<sup>[7]</sup> In the course of electrolysis sharp isosbestic points were observed, and the quantitative reproduction of the spectra of  $\text{MV}^{+}$  and  $\text{MV}^0$  on reoxidation proves the stability of  $\text{MV}^{+}$  and  $\text{MV}^0$  under the conditions employed.

Figure 2 shows spectral changes upon electrochemical oxidation ( $1.07$  V) and reduction ( $-1.83$  V) of  $[\text{Ru}(\text{bpy})_3]^{2+}$ . Oxidation to  $[\text{Ru}(\text{bpy})_3]^{3+}$  results in bleaching over the whole visible region, and increases in absorbance occur only below  $330\text{ nm}$ , while reduction to  $[\text{Ru}(\text{bpy})_3]^{+}$  gives rise to increased absorption around  $550$  and  $350\text{ nm}$ .

The spectral changes observed for the dyad upon the corresponding interconversions of the methyl viologen moiety ( $\text{MV}^{2+} \rightarrow \text{MV}^{+} \rightarrow \text{MV}^0$ ,  $-0.83\text{ V}$ ,  $-1.28\text{ V}$ ) and the  $\text{Ru}(\text{bpy})_3^{2+}$  moiety ( $[\text{Ru}(\text{bpy})_3]^{2+} \rightarrow [\text{Ru}(\text{bpy})_3]^{+}$ ,  $[\text{Ru}(\text{bpy})_3]^{2+} \rightarrow [\text{Ru}(\text{bpy})_3]^{3+}$ ,  $-1.80\text{ V}$ ,  $1.07\text{ V}$ ) are essentially identical to those observed with free methyl viologen and

Table 1. Electrochemical data.

Compounds <sup>[a]</sup>	$[\text{Ru}(\text{bpy})_3]^{0/-}$	$[\text{Ru}(\text{bpy})_3]^{+/0}$	$E_{1/2}$ [V] <sup>[b]</sup> ( $\Delta E_p$ [mV]) <sup>[c]</sup>		$\text{MV}^{2+/+}$	$[\text{Ru}(\text{bpy})_3]^{3+/2+}$
			$[\text{Ru}(\text{bpy})_3]^{2+/+}$	$\text{MV}^{+/0}$		
$\text{Ru}(\text{bpy})_3^{2+}$ – $\text{MV}^{2+}$	–2.180 (80)	–1.920 (66)	–1.730 (54)	–1.060 (57)	–0.665 (69)	0.905 (79)
$[\text{Ru}(\text{bpy})_3]^{2+}$	–2.180 (123)	–1.915 (72)	–1.725 (69)			0.895 (73)
$\text{MV}^{2+}$				–1.210 (68)	–0.820 (75)	

[a] As  $\text{PF}_6^-$  salts. [b] Versus  $\text{Fc}^+/\text{Fc}$  in  $\text{CH}_3\text{CN}$  solution with  $0.1\text{ M } [\text{N}(\text{nC}_4\text{H}_9)_4]\text{PF}_6$  as supporting electrolyte,  $\pm 0.02\text{ V}$ . [c]  $v = 50\text{ mV s}^{-1}$ .

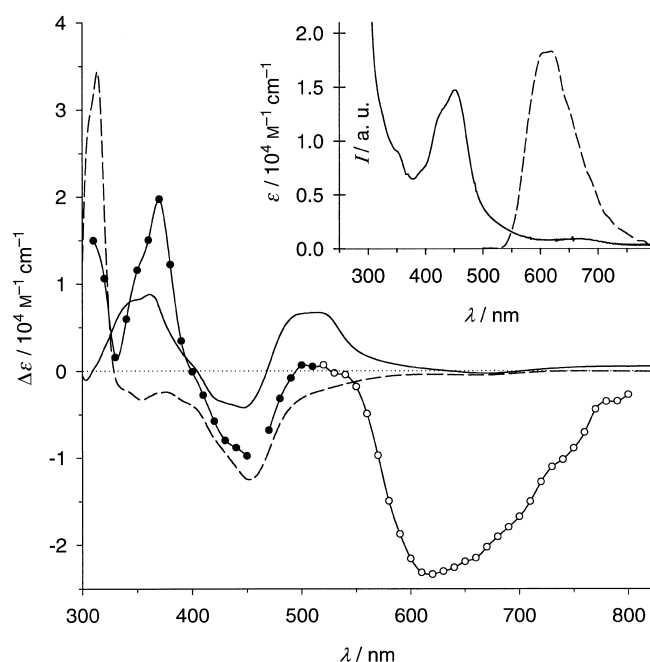


Figure 2. Difference absorption spectra of  $[\text{Ru}(\text{bpy})_3]^{3+}$  (---),  $[\text{Ru}(\text{bpy})_3]^{2+}$  (—), and  $^*[\text{Ru}(\text{bpy})_3]^{2+}$  (●) relative to  $[\text{Ru}(\text{bpy})_3]^{2+}$ . Emission from  $^*[\text{Ru}(\text{bpy})_3]^{2+}$  (○). Spectra were recorded in  $\text{CH}_3\text{CN}$  (0.1 M  $[\text{N}(\text{nC}_4\text{H}_9)_4]\text{PF}_6$ ) by spectroelectrochemistry (1.07 V and –1.83 V vs  $\text{Fc}^+/\text{Fc}$ ) and by laser flash photolysis ( $\lambda_{\text{ex}} = 460$  nm) of  $[\text{Ru}(\text{bpy})_3](\text{PF}_6)_2$ . Inset: Ground-state absorption (—) and excited state emission spectrum (---) of  $[\text{Ru}(\text{bpy})_3]^{2+}$ .

$[\text{Ru}(\text{bpy})_3]^{2+}$  model compounds. Maxima of all absorption bands agree within  $\Delta\lambda_{\text{max}} = 4$  nm, and a significant difference in extinction coefficients was found only for the 600 nm band of  $\text{MV}^{2+}$  ( $\epsilon_{608} = 16600 \text{ M}^{-1} \text{ cm}^{-1}$  for  $[\text{Ru}(\text{bpy})_3]^{2+} - \text{MV}^{2+}$ ,  $\epsilon_{605} = 13000 \text{ M}^{-1} \text{ cm}^{-1}$  for  $\text{MV}^{2+}$ ). Sharp isosbestic points were observed in the spectra obtained during all interconversions and the reverse processes.

**Bimolecular electron transfer:** Figure 2 shows a transient spectrum of  $[\text{Ru}(\text{bpy})_3]^{2+}$  taken immediately after the exciting nanosecond laser pulse at 460 nm. The spectrum shows an absorption of the  $^3\text{MLCT}$  state of  $[\text{Ru}(\text{bpy})_3]^{2+}$  with the maximum at 370 nm ( $\epsilon = 21600 \text{ M}^{-1} \text{ cm}^{-1}$ ,  $\Delta\epsilon = 17400 \text{ M}^{-1} \text{ cm}^{-1[9]}$ ) and a bleaching of the ground state absorption around 450 nm ( $\epsilon = 14700 \text{ M}^{-1} \text{ cm}^{-1}$ ,  $\Delta\epsilon = 10000 \text{ M}^{-1} \text{ cm}^{-1[9]}$ ), together with the emission peaking at 610 nm.

Electron-transfer reactions between excited  $[\text{Ru}(\text{bpy})_3]^{2+}$  and different redox forms of methyl viologen in acetonitrile solution were studied by electrochemical generation of the latter in the optical cell prior to flash photolysis. The resulting flash-generated transient spectra and some transient absorption traces are shown in Figure 3.

Without an applied potential  $^*[\text{Ru}(\text{bpy})_3]^{2+}$  is quenched by  $\text{MV}^{2+}$  to give the transient spectrum shown in Figure 3a. The spectrum can be assigned to the electron-transfer products of the well-known oxidative quenching reaction<sup>[1]</sup> [Scheme 1,

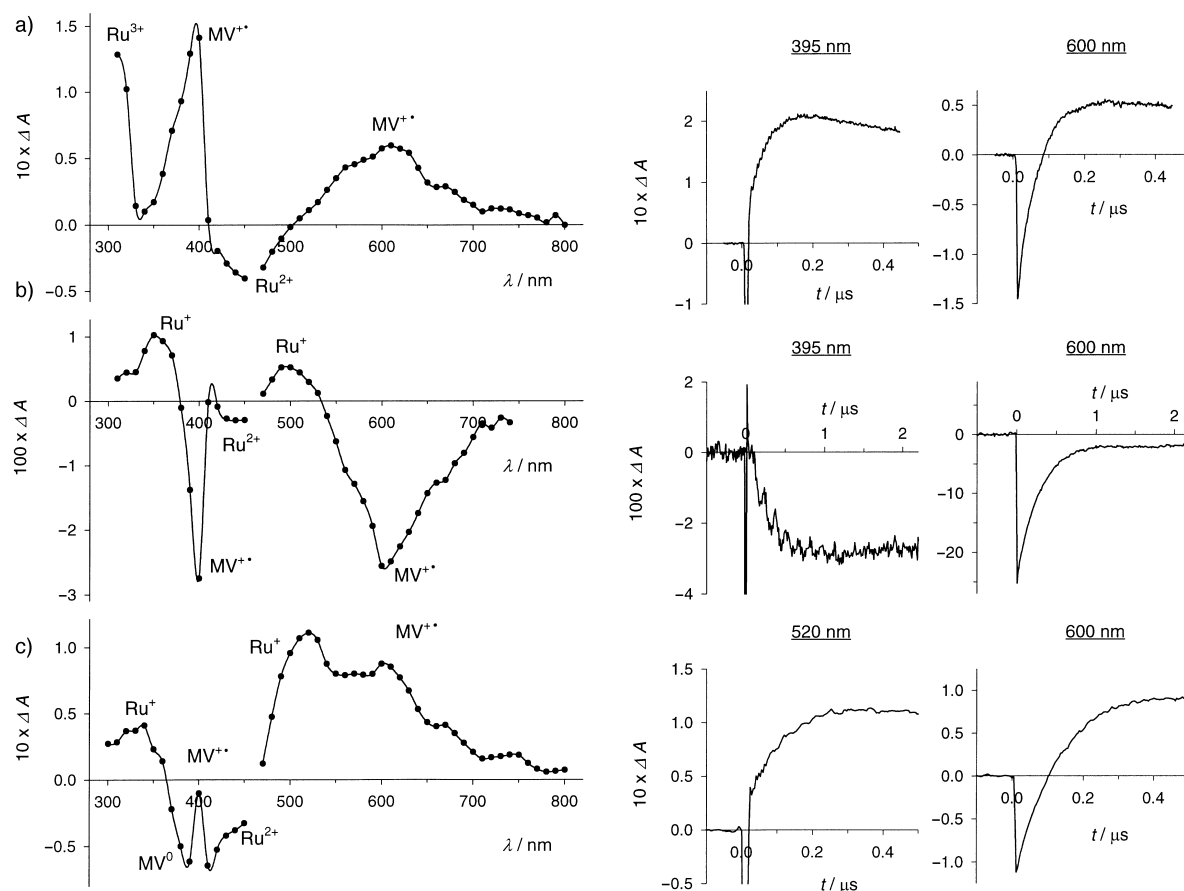
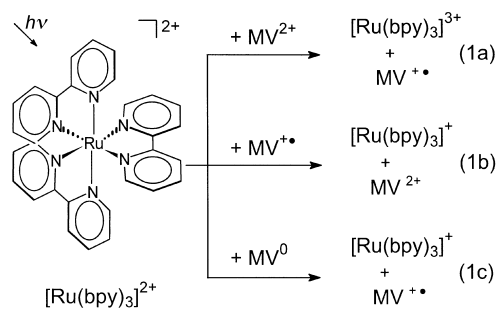


Figure 3. Transient spectra (left panel) and absorption traces (right panel) for the bimolecular reactions of  $^*[\text{Ru}(\text{bpy})_3]^{2+}$  with  $\text{MV}^{n+}$  in  $\text{CH}_3\text{CN}$  (0.1 M  $[\text{N}(\text{nC}_4\text{H}_9)_4]\text{PF}_6$ ). a)  $\text{MV}^{2+}$  (5 mM) at 400 ns, b)  $\text{MV}^{+}$  (–1.03 V, 0.2 mM) at 1  $\mu\text{s}$ , c)  $\text{MV}^0$  (–1.48 V, 0.4 mM) at 400 ns after the laser pulse.



Scheme 1. Quenching of the excited state of  $[\text{Ru}(\text{bpy})_3]^{3+}$  by MV species in bimolecular reactions.

reaction (1a)], that is,  $\text{MV}^{\bullet+}$  with absorption bands around 400 and 600 nm and  $[\text{Ru}(\text{bpy})_3]^{3+}$  absorbing below 350 nm, together with bleaching around 450 nm due to the depletion of  $[\text{Ru}(\text{bpy})_3]^{2+}$ .<sup>[10]</sup> The transient traces show the generation of strong absorption from  $\text{MV}^{\bullet+}$  at 395 and 600 nm. The initial bleach at 600 nm is due to  $^*[\text{Ru}(\text{bpy})_3]^{2+}$  emission.

When methyl viologen was reduced electrochemically to  $\text{MV}^{\bullet+}$  prior to laser flashing, the reaction with  $^*[\text{Ru}(\text{bpy})_3]^{2+}$  resulted in the transient absorption spectra shown in Figure 3b. The spectrum shows the bleached absorption bands of  $\text{MV}^{\bullet+}$  and  $[\text{Ru}(\text{bpy})_3]^{2+}$  together with positive absorption around 350 and 500 nm due to the formation of  $[\text{Ru}(\text{bpy})_3]^{3+}$ . This is clear evidence that the reaction with  $\text{MV}^{\bullet+}$  represents reductive quenching [Scheme 1, reaction (1b)]. In particular, the bleaching at 400 nm due to consumption of  $\text{MV}^{\bullet+}$  excludes oxidative quenching, since the absorption of  $\text{MV}^0$  generated in that case would completely compensate for this bleaching (see Figure 1, inset). The transient traces show the disappearance of  $\text{MV}^{\bullet+}$  absorptions at 395 and 600 nm. After the initial bleach at 600 nm due to  $^*[\text{Ru}(\text{bpy})_3]^{2+}$  emission, the absorption after excited-state decay is still much smaller than that prior to the laser flash. A positive absorption around 510 nm grows in with the same kinetics as the excited-state decay (not shown), and is attributed to reduced  $[\text{Ru}(\text{bpy})_3]^+$  (see spectrum Figure 3b).

Figure 3c shows a transient spectrum observed after reaction of electrochemically generated  $\text{MV}^0$  with  $^*[\text{Ru}(\text{bpy})_3]^{2+}$ , and it is consistent with the reductive electron-transfer mechanism [Scheme 1, reaction (1c)]. The positive absorption can be assigned to the formation of  $[\text{Ru}(\text{bpy})_3]^+$  and  $\text{MV}^{\bullet+}$ , while the bleaching can be attributed to the depletion of  $[\text{Ru}(\text{bpy})_3]^{2+}$  and  $\text{MV}^0$ . This is compensated at 400 nm by the absorption of  $\text{MV}^{\bullet+}$ , as shown by the narrow absorption peak superimposed on a broader bleach. The transient traces show the buildup of a positive absorption from  $[\text{Ru}(\text{bpy})_3]^+$  and  $\text{MV}^{\bullet+}$  at 520 nm and 600 nm, respectively.

In the absence of methyl viologen the  $^*[\text{Ru}(\text{bpy})_3]^{2+}$  excited state decays with  $k_0 = 1.9 \times 10^6 \text{ s}^{-1}$ . This is somewhat faster than typical literature values ( $1.1 \times 10^6 \text{ s}^{-1}$ )<sup>[11]</sup> owing to self-quenching by the relatively high concentration of  $[\text{Ru}(\text{bpy})_3]^{2+}$  required by the short path length of the OTTLE cell. Rate constants of the quenching reactions ( $k_q$ ) with methyl viologen ( $\text{MV}^{2+}$ ,  $\text{MV}^{\bullet+}$ , and  $\text{MV}^0$ ) were determined from the emission decay rates ( $k_{\text{obs}}$ ) observed for different concentrations of methyl viologen electrolyzed at different potentials (Figure 4). In all cases, the emission decay rate

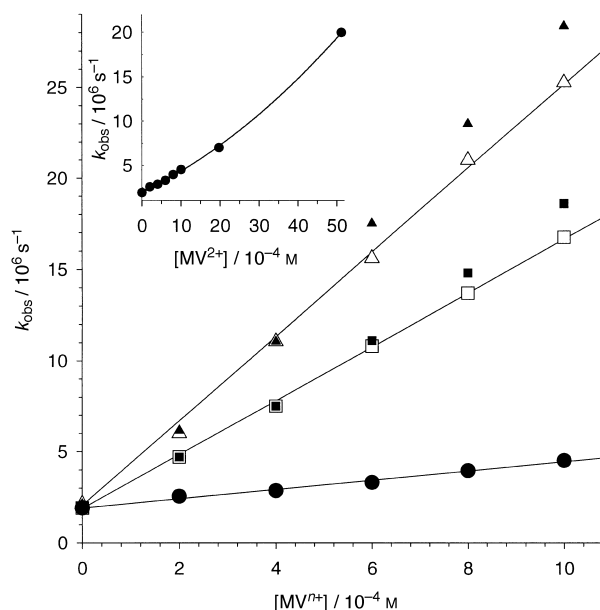


Figure 4. Pseudo-first-order rate constants ( $k_{\text{obs}}$ ) of emission decay from  $^*[\text{Ru}(\text{bpy})_3]^{2+}$  versus concentration of  $\text{MV}^{2+}$  (circles),  $\text{MV}^{\bullet+}$  (squares) and  $\text{MV}^0$  (triangles) in  $\text{CH}_3\text{CN}$  (0.1 M  $[\text{N}(\text{nC}_4\text{H}_9)_4]\text{PF}_6$ ). Values obtained from fits to 600 nm traces starting at  $t=0$  (filled symbols) or  $t=40 \text{ ns}$  (open symbols). Inset:  $k_{\text{obs}}$  vs concentration of  $\text{MV}^{2+}$  for  $[\text{MV}^{2+}] > 1 \text{ mM}$ .

constant agreed with those obtained from transient absorption traces over the whole spectrum. With increasing concentration of methyl viologen, the emission decay traces show increasing deviation from single exponential behavior for  $\text{MV}^{\bullet+}$  and  $\text{MV}^0$  and the pseudo-first-order plots of  $k_{\text{obs}}$  versus  $[\text{MV}^n+]$  show positive curvature for all viologen forms. Deviation from pseudo-first-order kinetics is moderate with  $\text{MV}^{2+}$ , but more pronounced with  $\text{MV}^{\bullet+}$  and  $\text{MV}^0$ . Nonlinear pseudo-first-order plots have been attributed to increasing  $k_q$  due to increasing ionic strength or due to ion pairing with the counterion.<sup>[12]</sup> In our case, however, none of these effects can account for the observed nonlinearities, since ionic strength and ion-pairing environment should not vary with increasing concentration of methyl viologen up to 1 mM due to the excess of supporting electrolyte (0.1 M  $[\text{N}(\text{nC}_4\text{H}_9)_4]\text{PF}_6$ ) and the use of  $\text{PF}_6^-$  salts of  $[\text{Ru}(\text{bpy})_3]^{2+}$  and  $\text{MV}^{2+}$ . Furthermore, cage-escape yields were found to increase with increasing concentration (see below), and this can not be explained by any of the aforementioned effects. Note also that we did not observe any contribution of  $(\text{MV}^{\bullet+})_2$  dimers under these conditions in the spectroelectrochemistry. Finally, “quenching sphere-of-action”,<sup>[13]</sup> that is, transient effects<sup>[14]</sup> cannot account for the nonlinearities at the moderate concentrations (ca. 1 mM) employed and the long timescale involved. It seems that a simple bimolecular scheme is not quantitatively correct at higher concentrations; nevertheless, linear pseudo-first-order plots were obtained by using rate constants from fits of the slower part of the traces by ignoring the first 40 ns of the decay amplitude. The values of  $k_q$  listed in Table 2 were obtained from these plots.

Values of  $k_q$  increase with increasingly negative free-energy changes (Table 2), as expected for reactions (1a) and (1b) from Marcus theory.<sup>[15]</sup> The further increase in  $k_q$  observed for

Table 2. Bimolecular quenching of  $^*[Ru(bpy)_3]^{2+}$  by  $MV^{n+}$ .<sup>[a]</sup>

Reaction	<i>n</i>	<i>k<sub>q</sub></i> [10 <sup>9</sup> M <sup>-1</sup> s <sup>-1</sup> ]	<i>k<sub>b</sub></i> <sup>[b]</sup> [10 <sup>10</sup> s <sup>-1</sup> ]	<i>k<sub>ce</sub></i> <sup>[c]</sup> [10 <sup>10</sup> s <sup>-1</sup> ]	<i>k<sub>rec</sub></i> [10 <sup>9</sup> M <sup>-1</sup> s <sup>-1</sup> ]	$\phi_{ce}$	$-\Delta G_{et}^{[d,e]}$ [eV]	$-\Delta G_b^{[e]}$ [eV]
1a	2	2.5	7.7	3.3	18.9	0.30	0.39	1.72
1b	1	15	9.2	2.3	7.7	0.2	1.20	0.91
1c	0	23	0.9	1.4	7.5	0.6	1.59	0.52

[a] As  $PF_6^-$  salts in  $CH_3CN$  solution with 0.1 M  $[N(C_4H_9)_4]PF_6$ . [b] Calculated from  $\phi_{ce}$  and  $k_{ce}$ . [c] Calculated with  $r = 10 \text{ \AA}$ .<sup>[19]</sup> [d] Calculated with  $E^* = 2.12 \text{ eV}$  (<sup>[11]</sup>). [e] Neglecting the coulombic work terms  $\Delta G_w^0(a) = \Delta G_w^0(c) = \pm 0.04 \text{ eV}$  (– for forward and + for back reactions, with  $r = 10 \text{ \AA}$ ),  $\Delta G_w^0(b) = 0$ .

reaction (1c), which can be expected to occur in the inverted Marcus region ( $\Delta G_b^0(1c) = -1.59 \text{ eV}$ ), must be attributed to effects on the diffusional rate constants, that is, the absence of coulombic repulsion between  $[Ru(bpy)_3]^{2+}$  and  $MV^0$  seems to more than compensate for the effect of driving force on the rate constant for forward electron transfer in the encounter complex.<sup>[16]</sup>

Quantum yields of electron-transfer products ( $\Phi_{et}$ ) were determined from absorbance changes at 610 nm ( $\Delta A_{610}$ ), which are due to the formation or depletion of  $MV^{+}$ . The  $\Phi_{et}$  values, which can be expressed as the product of quenching efficiency ( $f_q$ ) and the cage-escape yield of the electron-transfer products from the solvent cage ( $\phi_{ce}$ ), were calculated from the initial bleaching of the  $[Ru(bpy)_3]^{2+}$  ground state absorption at 450 nm ( $\Delta \epsilon_{450} = 10000 \text{ M}^{-1} \text{ cm}^{-1}$ )<sup>[9]</sup> as an internal actinometer.

With  $MV^{2+}$  a linear plot of  $\Phi_{et}$  versus  $f_q$  was obtained, and  $\phi_{ce}(1a) = 0.30$  was determined from the slope. This value is in agreement with earlier studies under comparable conditions.<sup>[17]</sup> With  $MV^{+}$  and  $MV^0$  the plots of  $\Phi_{et}$  versus  $f_q$  show strong positive curvature for  $f_q > 0.7$ – $0.8$ , corresponding to  $[MV^{+}] > 0.6$  and  $[MV^0] > 0.4 \text{ mM}$ , respectively (not shown). Values of  $\phi_{ce}(1b) = 0.2$  and  $\phi_{ce}(1c) = 0.6$  were estimated from the limiting tangents of the curves for  $f_q \rightarrow 0$  and are given in Table 2.

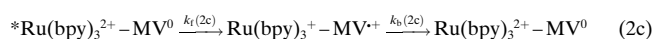
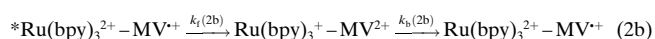
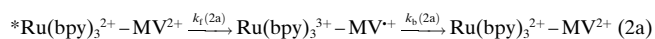
Values of  $\phi_{ce}$  have been reported to be only weakly dependent on  $\Delta G_b^0$  in bimolecular reactions involving  $Ru^{II}$  sensitizers.<sup>[18]</sup> In the present case, however, the effect of coulombic interaction of the differently charged electron-transfer products on the rate constants of cage escape ( $k_{ce}$ ) would result in  $k_{ce}(1a) > k_{ce}(1b) > k_{ce}(1c)$ , which cannot account for the observed differences in cage-escape yields. Instead the higher values of  $\phi_{ce}$  for reactions (1a) and (1c) relative to reaction (1b) probably reflect significant differences in the rate constants of back electron transfer ( $k_b$ ), which may be qualitatively explained by the differences in  $\Delta G^0$  of back electron transfer. Values of  $k_b$  were estimated (Table 2) from the measured values of  $\phi_{ce}$  and values of  $k_{ce}$  calculated with the Eigen equation with an assumed distance of  $r \approx 10 \text{ \AA}$ <sup>[19]</sup> between the redox products in the solvent cage. The relative values of  $k_b$  follow a Marcus free-energy relationship, reaching a maximum for reaction (1b) at  $\Delta G_b^0(1b) = -0.91 \text{ eV}$ , and decreasing again for reaction (1a), which would be in the inverted region ( $\Delta G_b^0(1a) = -1.72 \text{ eV}$ ).<sup>[16]</sup>

The rate constants for bimolecular recombination of the electron-transfer products that had escaped into the bulk ( $k_{rec}$ ) were determined from second-order fits to 610 nm traces monitoring the decay of  $MV^{+}$ . While  $k_{rec}(1a)$  is almost diffusion-controlled,  $k_{rec}(1b)$  and  $k_{rec}(1c)$  are somewhat slow-

er. The order  $k_{rec}(1a) > k_{rec}(1b) \approx k_{rec}(1c)$  is the opposite to what is expected from coulombic effects on the diffusional constants, and this suggests that the higher value for reaction (1a) is due to a faster electron-transfer step. This may be rationalized by a larger effective reaction distance for an inverted-region reaction<sup>[20]</sup> or by the difference in electronic states involved.<sup>[16]</sup>

In addition to the effect of  $\phi_{ce}$ , a competition between electron and energy transfer might affect  $\Phi_{et}$ . While energy transfer from  $^*[Ru(bpy)_3]^{2+}$  to  $MV^{2+}$  can be excluded for thermodynamic reasons ( $E^*(MV^{2+}) = 3.10 \text{ eV}$ <sup>[21]</sup>), Förster-type energy transfer to  $MV^{+}$  seems favorable due to the spectral overlap, and its contribution to the bimolecular quenching of  $^*[Ru(bpy)_3]^{2+}$  by  $MV^{+}$  can not be excluded. For the emission of  $^*[Ru(bpy)_3]^{2+}$  and the absorption of  $MV^{+}$  an overlap integral of  $J = 1.1 \times 10^{-13} \text{ M}^{-1} \text{ cm}^3$  was calculated.<sup>[22]</sup> Taking the distance of  $r = 9 \text{ \AA}$  that was determined for the dyad,<sup>[6]</sup> which is also a reasonable value for the contact distance in the bimolecular reaction, an upper limit of the rate of Förster-type energy transfer of  $k_{FE} = 9 \times 10^9 \text{ s}^{-1}$  can be estimated with a refractive index of  $n = 1.342$ , an emission quantum yield of  $\Phi_d = 0.04$ ,<sup>[23]</sup> a donor lifetime of  $\tau_d = 10^{-6} \text{ s}$ , and an orientation factor of  $\kappa^2 \leq 4$ . This indicates that energy transfer to give the short-lived excited  $MV^{+}$  (see below) cannot be excluded as a quenching mechanism parallel to electron transfer in the bimolecular reaction. The results from the dyad (see below) show, however, that energy transfer is insignificant relative to the rapid electron transfer in the intramolecular reaction.

**Electron transfer in the  $Ru(bpy)_3^{2+}$ – $MV^{n+}$  dyads:** The electron-transfer reactions in the covalently linked  $Ru(bpy)_3^{2+}$ – $MV^{n+}$  dyad in acetonitrile solution were studied with femtosecond pump–probe spectroscopy. Basically the same picture as drawn for the bimolecular reactions holds for the course of the intramolecular electron transfer, but without the complications from diffusional reaction steps. The initial electron-transfer quenching of the  $^*[Ru(bpy)_3]^{2+}$  moiety changes from oxidative with  $MV^{2+}$  to reductive in the case of  $MV^{+}$  and  $MV^0$ . Features of the electron-transfer products appear in the transient absorption spectra (Figure 5). The transient absorption traces are consistent with the consecutive reactions (2a)–(2c), and a few examples are given in Figure 5 (right panel). The transient absorption  $\Delta A$  at different probe wavelengths as a function of the delay time  $t$  between pump and probe pulses was fitted to consecutive first-order reactions (2a–c). A summary of the rate constants obtained at the three different potentials applied is given in Table 3.



**The  $Ru(bpy)_3^{2+}$ – $MV^{2+}$  dyad:** Figure 5a shows a spectrum of  $Ru(bpy)_3^{2+}$ – $MV^{2+}$  10 ps after excitation of the  $[Ru(bpy)_3]^{2+}$  moiety at 460 nm, with no potential applied to the cell. Besides the bleaching of the ground state of  $[Ru(bpy)_3]^{2+}$

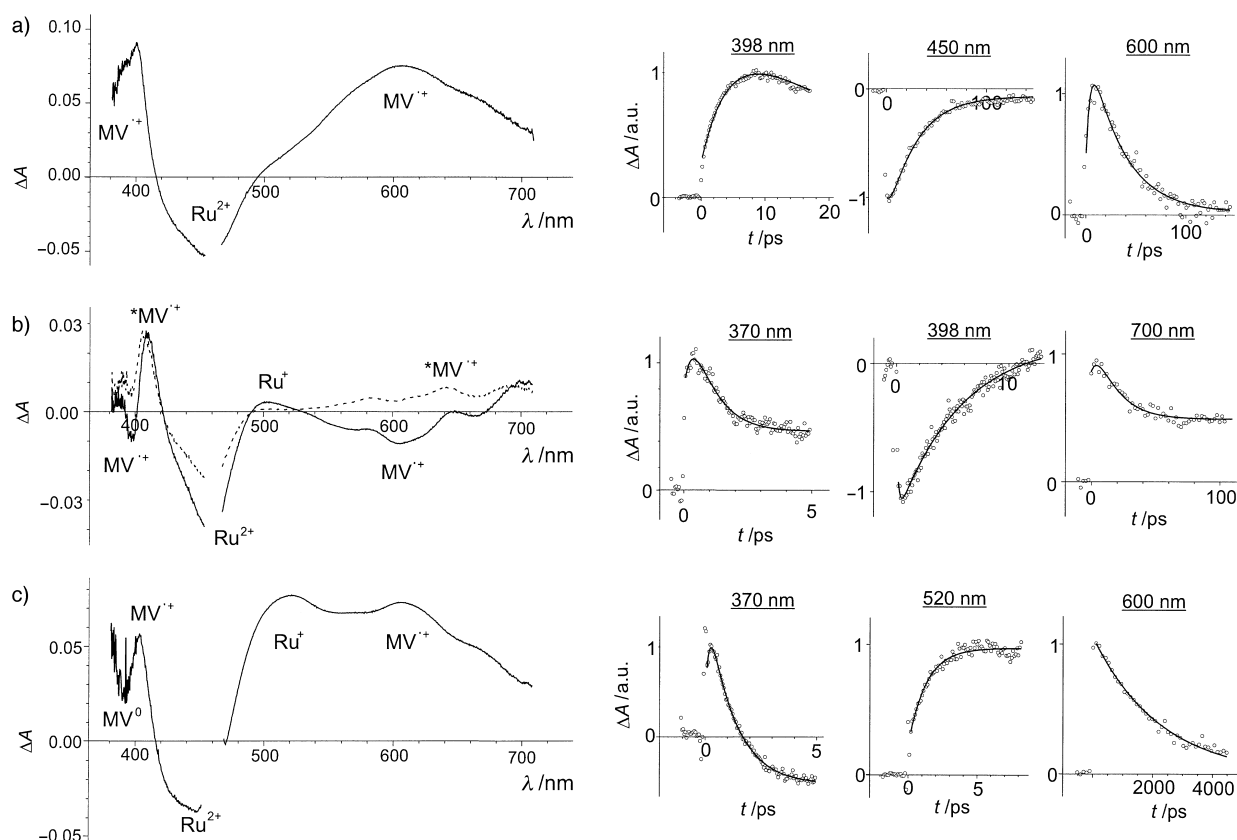


Figure 5. Transient spectra (left) and absorption traces (right) for the intramolecular reactions in the  $^*\text{Ru}(\text{bpy})_3^{2+}-\text{MV}^{n+}$  dyad in  $\text{CH}_3\text{CN}$  (0.1 M  $[\text{N}(\text{C}_4\text{H}_9)_4]\text{PF}_6$ ). a)  $^*\text{Ru}(\text{bpy})_3^{2+}-\text{MV}^{2+}$ , 10 ps; b)  $^*\text{Ru}(\text{bpy})_3^{2+}-\text{MV}^{+}$  ( $-0.88$  V), 3 ps (—), and 10 ps (---;  $^*\text{MV}^{+}$  refers to the vibrationally excited state); and c)  $^*\text{Ru}(\text{bpy})_3^{2+}-\text{MV}^0$  ( $-1.28$  V) 5 ps after the laser pulse.

Table 3. Intramolecular quenching in  $^*\text{Ru}(\text{bpy})_3^{2+}-\text{MV}^{n+}$ .<sup>[a]</sup>

Reaction	$n$	$k_f$ [ $10^{10}\text{s}^{-1}$ ]	$k_b$ [ $10^{10}\text{s}^{-1}$ ]	$-\Delta G_f^{\text{p[b]}}$ [eV]	$-\Delta G_b^{\text{p[b]}}$ [eV]
2a	2	25	3.3	0.53	1.57
2b	1	130	17	1.04	1.07
2c	0	83	0.046	1.43	0.67

[a] As  $\text{PF}_6^-$  salt in  $\text{CH}_3\text{CN}$  solution with 0.1 M  $[\text{N}(\text{C}_4\text{H}_9)_4]\text{PF}_6$ . [b] Neglecting the coulombic work terms  $\Delta G_w^0(\text{a}) = \Delta G_w^0(\text{c}) = \pm 0.04$  eV ( $-$  for forward and  $+$  for back reactions, with  $r = 9$  Å),<sup>[6]</sup>  $\Delta G_w^0(\text{b}) = 0$ .

moiety around 450 nm, increases in absorption at 400 nm and around 600 nm are observed that can be assigned to the formation of  $\text{MV}^{+}$  by oxidative quenching of the  $^3\text{MLCT}$  state of  $[\text{Ru}(\text{bpy})_3]^{2+}$ , in agreement with conclusions for similar dyads.<sup>[6]</sup> Plots of the absorption change versus the delay between pump and probe pulses for three informative wavelengths are shown next to the spectrum. The traces at 398 and 600 nm both evolve with the same kinetics due to formation ( $\tau_f = 4.5 \pm 0.5$  ps) and decay ( $\tau_b = 30 \pm 2$  ps) of the radical ion  $\text{MV}^{+}$ . The bleach magnitudes at 450 nm for the excited and oxidized  $[\text{Ru}(\text{bpy})_3]^{2+}$  moieties are nearly identical. Thus, the trace at 450 nm follows the recovery of the  $[\text{Ru}(\text{bpy})_3]^{2+}$  ground state with the time constant of back electron transfer  $\tau_b$ . The back electron transfer with  $\Delta G_b^0(2\text{a}) = -1.57$  eV lies in the Marcus inverted region, as demonstrated by Yonemoto et al. for a series of  $\text{Ru}(\text{bpy})_3^{2+}-\text{MV}^{2+}$  dyads,<sup>[6]</sup> which are very similar to that investigated here.

**The  $\text{Ru}(\text{bpy})_3^{2+}-\text{MV}^{+}$  dyad:** The first reduction of methyl viologen in the dyad was carried out by electrolysis at  $-0.88$  V to generate the  $\text{Ru}(\text{bpy})_3^{2+}-\text{MV}^{+}$  form. Unlike the dication,  $\text{MV}^{+}$  acts as a reductant towards the  $[\text{Ru}(\text{bpy})_3]^{2+}$  moiety. The solid line in Figure 5b is the absorption change obtained 3 ps after the excitation, when the forward electron transfer is complete. Significant bleaching of the  $\text{MV}^{+}$  absorptions are observed just below 400 nm and around 600 nm, while the  $[\text{Ru}(\text{bpy})_3]^{2+}$  bleaching around 450 nm and the absorption at 500 nm can be attributed to formation of an  $[\text{Ru}(\text{bpy})_3]^+$  moiety. The time profiles to the right of the spectra in Figure 5b contain the following information: the absorption at 370 nm is due to the  $^3\text{MLCT}$  state of the  $[\text{Ru}(\text{bpy})_3]^{2+}$  moiety. Fast pulse-limited formation is followed by  $300 \pm 100$  fs of further development, presumably due to initial excited-state relaxation.<sup>[24]</sup> The subsequent decay can be attributed to forward electron transfer with a time constant of  $\tau_f = 800 \pm 100$  fs, since bleaching of the  $\text{MV}^{+}$  absorptions at 600 and 398 nm, as well as  $[\text{Ru}(\text{bpy})_3]^+$  absorption at 502 nm (not shown) appear with the same time constant. The signal at 370 nm levels off at about 50% of its initial value, since the  $[\text{Ru}(\text{bpy})]^+$  state also has a strong absorption at this wavelength. The back electron transfer can be monitored by the disappearance of the  $\text{MV}^{+}$  bleach, with a time constant of  $\tau_b = 5.7 \pm 0.3$  ps.

However, excitation at 460 nm generates not only the  $^3\text{MLCT}$  state of  $[\text{Ru}(\text{bpy})_3]^{2+}$  moiety. Although the extinction coefficient of  $\text{MV}^{+}$  at 460 nm is small (ca.  $1000\text{M}^{-1}\text{cm}^{-1}$ ),

some direct excitation of  $MV^{++}$  causes a positive transient absorption with maxima slightly above 400 nm and at 585, 640, and 700 nm. This is seen most clearly 10 ps after excitation, when the parallel electron-transfer reaction is almost complete (Figure 5b, dashed line), but the spectral structure of the longer lived species is already observable just after excitation. The spectrum resembles the absorption of  $MV^{++}$  but is red-shifted by about  $810\text{ cm}^{-1}$ , which equals the energy of the lowest intraring C–C stretching mode of  $MV^{++}$ .<sup>[25]</sup> The lifetime of this species is  $15 \pm 1\text{ ps}$  (see trace probed at 700 nm, Figure 5b). As shown in Figure 6, the same

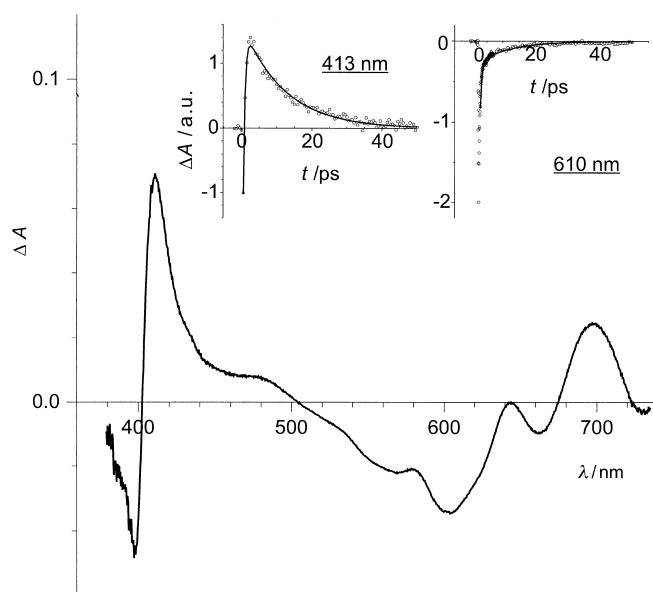


Figure 6. Transient spectrum (5 ps) and absorption traces (insets) for the excitation of  $Ru(bpy)_3^{2+}-MV^{++}$  at 600 nm in  $CH_3CN$  ( $0.1\text{ M }[N(nC_4H_9)_4]PF_6$ ).

transient is observed 5 ps after exciting only the  $MV^{++}$  moiety of the dyad at 600 nm. The transient absorption, as monitored in the trace at 413 nm, is formed within  $500 \pm 100\text{ fs}$  and decays with a time constant of  $15 \pm 1\text{ ps}$ . In a previous time-resolved resonance Raman study of  $MV^{++}$  in water it was concluded that a vibrationally excited ground state of  $MV^{++}$  was formed within 350 fs after excitation at 379.5 nm, and decayed with  $\tau = 2\text{ ps}$ .<sup>[26]</sup> We observe similar dynamics in acetonitrile, and the new absorption features have the expected appearance of a ground state of  $MV^{++}$  with one additional vibrational quantum of about  $810\text{ cm}^{-1}$ . Hence, we attribute this species to the lowest vibrationally excited ground state of  $MV^{++}$ .

Quenching of the excited  $[Ru(bpy)_3]^{2+}$  moiety by energy transfer in parallel to electron transfer may be conceivable because of the large spectral overlap between the  $*[Ru(bpy)_3]^{2+}$  emission and the  $MV^{++}$  absorption. Although Förster-type energy transfer would be at least two orders of magnitude too slow to compete ( $k_{FE} = 9 \times 10^9\text{ s}^{-1}$ , see above), Dexter-type energy transfer is possible. However, no additional formation of excited  $MV^{++}$  with the same kinetics as  $*[Ru(bpy)_3]^{2+}$  decay was observed, and this leads us to the conclusion that energy-transfer quenching is not significant in the dyad.

Within 100 ps the reactions in the dyad are complete. A long-lived absorption remains throughout the whole spectrum, which can be assigned to the excited  $[Ru(bpy)_3]^{2+}$  moiety in dyads in which the viologen moiety had decomposed during measurements. In the femtosecond pump–probe experiments it appears as a constant background. Its spectrum was recorded after 100 ps (not shown) and subtracted from those presented in Figure 5b. The uncertainty in this procedure can explain the unexpected magnitude of ground-state bleaching at 450 nm in the spectrum 10 ps after excitation, and the long-lived absorption at the end of the 700 nm traces (Figure 5b). The time profile taken at 450 nm does not show any indication of additional transients. The slow degradation of the dyad was confirmed by a strong increase in steady state emission measured after 6 h of continued irradiation of a reduced sample. Reaction with oxygen reduction products from residual traces of dioxygen has been reported to be responsible for the loss of the electron-transfer quenching ability of the viologen moiety in linked  $Ru(bpy)_3^{2+}$ –viologen species.<sup>[27]</sup> In our case, however, no change of the UV/Vis absorption spectrum was observed when the reduced dyad was kept for 5 h in the argon-flushed spectroelectrochemical cell at  $-0.88\text{ V}$ , that is, under the conditions employed for the fs measurements but without irradiation. This result indicates that reactive oxygen species are not formed efficiently from residual dioxygen ( $O_2 + e^- \rightarrow O_2^{\cdot-}$ ,  $E_{1/2} = -1.18\text{ V}$ <sup>[28]</sup>) under these conditions, and we suggest that photoreactions of the reduced dyad account for the observed degradation.

**The  $Ru(bpy)_3^{2+}-MV^0$  dyad:** The methyl viologen moiety in the dyad was reduced to its neutral form at  $-1.28\text{ V}$ . Figure 5c shows the transient spectrum 5 ps after excitation. The characteristic absorption of  $MV^{++}$  appears around 600 nm. Around 400 nm both  $MV^0$  and  $MV^{++}$  have a similarly strong absorption, and absorption changes remain moderate, although the  $MV^{++}$  peak at 400 nm is apparent. Another characteristic band with a maximum around 520 nm can be attributed to the absorption of the  $[Ru(bpy)_3]^+$  moiety. The kinetic traces recorded at 370 nm ( $*[Ru(bpy)_3]^{2+}$ ) and 520 nm ( $[Ru(bpy)_3]^+$ ) show excited-state decay and product formation with a time constant of  $\tau_f = 1.2 \pm 0.1\text{ ps}$ . The fast initial rise ( $200 \pm 100\text{ fs}$ ) at 370 nm again shows the relaxation in the excited  $^3MLCT$  state.<sup>[24]</sup> The positive transient absorption change at 370 nm turns into a negative signal due to a smaller absorption of  $MV^{++}$  compared to  $MV^0$ . The back electron transfer is very slow ( $\tau_b = 2.1 \pm 0.1\text{ ns}$ ), as can be seen from the decay of the  $MV^{++}$  absorption at 600 nm (Figure 5c).

**Comparison between the redox forms of the dyad:** The relative values of the forward and backward electron-transfer rate constants (Table 3) in the different forms of the dyad follow qualitatively the free-energy relationship predicted by Marcus,<sup>[15]</sup> reaching their maximum value in the  $Ru(bpy)_3^{2+}-MV^{++}$  dyad, for which  $\Delta G_i^0(2b)$  and  $\Delta G_b^0(2b)$  are both about  $-1.0\text{ eV}$ . As for the bimolecular reactions above, however, comparisons based only on free energy are not necessarily correct.<sup>[16]</sup> This is most clearly exemplified by the about 400-fold slower back reaction in  $Ru(bpy)_3^+-MV^0$  [reaction (2c)]

compared to  $\text{Ru}(\text{bpy})_3^{2+} - \text{MV}^{+\bullet}$  [reaction (2b)]. The difference is much too large to be explained by an increase in activation energy.<sup>[29]</sup> In addition to the different viologen states involved, the viologen might affect the localization of the excess electron in the  $[\text{Ru}(\text{bpy})_3]^+$  moiety. The electron is localized on one bipyridine ligand at any time,<sup>[11]</sup> and back electron transfer presumably occurs when it is transiently located on the ligand that forms a bridge to the viologen moiety, as has been deduced for the forward electron transfer from  $^*[\text{Ru}(\text{bpy})_3]^{2+}$  moiety in other Ru–quencher dyads.<sup>[30]</sup> When the viologen moiety is reduced, as in the back reaction [reaction (2c)], it will increase the electron density on the bridging bipyridine ligand and shift the excess electron towards the remote ligands. This could explain the much smaller reaction rate compared to the case of reaction (2b).

In the lowest <sup>3</sup>MLCT excited state of  $[\text{Ru}(\text{bpy})_3]^{2+}$ , the electron is localized on one ligand, giving formally  $[\text{Ru}^{\text{III}}(\text{bpy})_2(\text{bpy}^{\bullet-})]$ .<sup>[11]</sup> The interligand hopping of the excitation in the homoleptic complex  $[\text{Ru}(\text{bpy})_3]^{2+}$  has been reported to occur with a time constant of about 75 ps in acetonitrile.<sup>[31]</sup> In the present dyad, excitation in the lowest MLCT absorption band around 460 nm can be expected to generate excited states on the three different ligands in equal proportions. However, in all the redox forms of the dyad, forward electron transfer from the excited state occurs with time constants of 4 ps or less. There is no sign of a difference in rate constant between complexes in which excitation is on the bridging or on the remote ligands. From the magnitude of the transient absorption from the electron-transfer products (Figure 5) it is clear that the entire  $^*[\text{Ru}(\text{bpy})_3]^{2+}$  population reacts with the same rate (e.g., compare the bleach at 450 and the absorption at 600 nm in Figure 5a). This indicates that interligand hopping in this heteroleptic complex is much faster than the observed forward electron transfer and, hence, occurs on a timescale of 1 ps or less, in contrast to the case of the  $^*[\text{Ru}(\text{bpy})_3]^{2+}$  complex.<sup>[31]</sup>

## Conclusion

Transient absorption spectroscopy on the nano- to femto-second timescale showed that quenching of the excited  $^*[\text{Ru}(\text{bpy})_3]^{2+}$  by  $\text{MV}^{+\bullet}$  and  $\text{MV}^0$  generates the reduced ruthenium complex and oxidizes the viologen, both in the bimolecular reaction and in the  $\text{Ru}(\text{bpy})_3^{2+} - \text{MV}^{n+}$  dyad. This is in contrast to the well-known oxidative quenching observed with  $\text{MV}^{2+}$  and shows that the direction of electron transfer in a  $\text{Ru}(\text{bpy})_3^{2+}$ –viologen molecular electronic device can be switched by an externally applied bias. Both the forward and back electron-transfer reactions in the  $\text{Ru}(\text{bpy})_3^{2+} - \text{MV}^{2+}$  and  $\text{Ru}(\text{bpy})_3^{2+} - \text{MV}^{+\bullet}$  dyads are rapid, with lifetimes between 0.8 and 30 ps. This demonstrates the potential of the dyad not only as a redox-switchable photodiode but also as a rapid photoswitchable unit when linked to a second chromophore. Competing quenching of the  $^*[\text{Ru}(\text{bpy})_3]^{2+}$  state by energy transfer to the  $\text{MV}^{+\bullet}$  radical could be ruled out for the dyad but may be significant in the bimolecular reaction. Direct excitation of the  $\text{MV}^{+\bullet}$  moiety in the  $\text{Ru}(\text{bpy})_3^{2+} - \text{MV}^{+\bullet}$  dyad generated a low-lying vibrationally excited state of the  $\text{MV}^{+\bullet}$

radical cation, with a lifetime of 15 ps, the absorption spectrum of which is red-shifted by approximately  $810\text{ cm}^{-1}$  compared to ground-state  $\text{MV}^{+\bullet}$ .

## Experimental Section

**Electrochemistry:** Cyclic voltammetry, differential pulse voltammetry, and controlled-potential electrolysis were carried out with an Autolab potentiostat with an GPES electrochemical interface (Eco Chemie). The working electrode was a glassy carbon disk (diameter 2 mm, freshly polished) for voltammetry, and a platinum grid for bulk electrolysis. A platinum spiral in a compartment separated from the bulk solution by a fritted disk was used as counterelectrode. The reference electrode was a nonaqueous  $\text{Ag}/\text{Ag}^+$  electrode (CH Instruments, 0.01M  $\text{AgNO}_3$  in acetonitrile) with a potential of  $-0.08\text{ V}$  versus the ferrocenium/ferrocene ( $\text{Fc}^+/\text{Fc}$ ) couple in acetonitrile as an external standard. All potentials reported here are versus the  $\text{Fc}^+/\text{Fc}$  couple by adding  $-0.08\text{ V}$  to the potentials measured versus the  $\text{Ag}/\text{Ag}^+$  electrode.

All solutions were prepared from dry acetonitrile (Merck, spectroscopy grade, dried with  $3\text{ \AA}$  molecular sieves) with 0.1M tetrabutylammonium hexafluorophosphate (Fluka, electrochemical grade, dried at 373 K) as supporting electrolyte. Glassware was oven dried, assembled, and flushed with argon while hot. Before all measurements, oxygen was removed by bubbling solvent-saturated argon through the stirred solutions, and the samples were kept under argon atmosphere during measurements.

**Spectroelectrochemistry:** Spectroelectrochemical measurements were made in a OTTLE-type quartz cell with an optical path length of 1 mm. A platinum grid of size  $10 \times 30\text{ mm}^2$  with 400 meshes per square centimeter was used as working electrode. The counter- and reference electrodes were of the same type as described for electrochemistry.

Solvent-saturated argon was bubbled through samples for 20 min, and they were then transferred to the argon-flushed cell with an argon stream.

The spectra were recorded on an UV/Vis diode array spectrophotometer (Hewlett Packard 8435); the background was collected on electrolyte solution in the potential-free OTTLE cell.

**Flash photolysis:** Nano- and microsecond transient absorption and emission measurements were obtained with a flash photolysis setup consisting of a Nd:YAG laser/optical parametric oscillator (OPO) combination (Quintel) and a flash photolysis spectrometer (Applied Photophysics). The samples were excited at 460 nm with 5 ns pulses of 15 mJ in the OTTLE cell, which was oriented at  $45^\circ$  relative to both the excitation and analyzing light, which were in a  $90^\circ$  cross-beam configuration. The samples contained  $[\text{Ru}(\text{bpy})_3](\text{PF}_6)_2$  (ca. 0.3 mm) to give an absorption of 0.45 in the 1 mm cell (0.63 at  $45^\circ$ ) at the excitation wavelength.  $\text{MV}(\text{PF}_6)_2$  was added to the samples from a concentrated stock solution to final concentrations of 0.2–5 mm. The concentration of  $\text{MV}(\text{PF}_6)_2$  was determined by spectrophotometry. Flash photolysis measurements on the same samples were carried out without applied potential and after exhaustive electrolysis at appropriate potentials to reduce the methyl viologen.

**Femtosecond pump–probe experiments:** These were carried out by using regenerative amplified pulses of a Ti:sapphire laser system (Coherent/Quantronix<sup>[32]</sup>: 120 fs pulse duration, central wavelength 800 nm, 1 kHz repetition rate). The excitation wavelength of 460 nm (2  $\mu\text{J}$  pulse energy) was generated by tripling the frequency of the signal wave of a tunable optical parametric amplifier (TOPAS). Transient absorption changes were probed by delayed white-light continuum pulses generated by the fundamental wave (800 nm) in a rotating  $\text{CaF}_2$  plate (thickness 5 mm) under magic-angle polarization and detected either as a lock-in amplified signal from a photomultiplier tube (PMT) at a certain probe wavelength or by recording whole spectra (380–740 nm) with a CCD camera connected to a spectrograph (Oriel). The spectral chirp was about 3 ps over 370–700 nm, which did not prohibit identification of the electron-transfer products.

The samples contained  $[\text{Ru}(\text{bpy})_3 - \text{MV}](\text{PF}_6)_4$  (ca. 0.20–0.27 mm), which resulted in an absorption of 0.3–0.4 in the 1 mm cell at the excitation wavelength. Measurements were carried out in the OTTLE cell without applied potential and after exhaustive electrolysis at appropriate potentials. The cell was moved vertically during measurements to minimize local heating effects. A slit in the working electrode allowed the laser beams to pass the cell without being scattered by the grid.

**Materials:**  $[\text{Ru}(\text{bpy})_3](\text{PF}_6)_2$  and  $\text{MV}(\text{PF}_6)_2$  were prepared from the commercially available chloride salts and were provided by L. Sun (Stockholm).

$[\text{Ru}(\text{bpy})_3-\text{MV}](\text{PF}_6)_4$ : The starting materials were prepared as described earlier.<sup>[33]</sup>  $[\text{Ru}(\text{bpy})_2(4\text{-BrCH}_2-4'\text{-CH}_3\text{-bpy})](\text{PF}_6)_2$  (0.350 g, 0.36 mmol) and 1-[(4'-methyl-2,2'-bipyridine-4-yl)methyl]-4,4'-bipyridinium bromide (0.150 g, 0.36 mmol) were heated to reflux in  $\text{CH}_3\text{CN}$  (20 mL) under nitrogen for 20 h. The solvent was evaporated in vacuo, and the residue was purified twice by chromatography on silica (eluent:  $\text{CH}_3\text{CN}/\text{H}_2\text{O}$ /satd  $\text{KNO}_3$ , 5:4:1). Excess  $\text{KNO}_3$  in fractions containing product was removed by dissolving the product as a nitrate salt in  $\text{CH}_3\text{CN}$  followed by filtration. The solvent was evaporated in vacuo, and the solid redissolved in a minimum amount of  $\text{H}_2\text{O}$  and precipitated by addition of a tenfold excess of  $\text{NH}_4\text{PF}_6$ . The orange solid was collected by filtration and washed repeatedly with several portions of  $\text{H}_2\text{O}$  and  $\text{Et}_2\text{O}$ , and dried under vacuum (0.092 g, 17%).  $R_f = 0.05$  ( $\text{CH}_3\text{CN}/\text{H}_2\text{O}$ /satd  $\text{KNO}_3$ , 5:4:1, silica gel);  $^1\text{H}$  NMR (400 MHz,  $[\text{D}_6]\text{acetone}$ , 25 °C, TMS):  $\delta = 9.63$  (d,  $J = 7.2$  Hz, 2H), 9.47 (d,  $J = 6.8$  Hz, 2H), 8.95 (d,  $J = 1.2$  Hz, 1H), 8.85 (d,  $J = 6.8$  Hz, 2H), 8.83–8.74 (m, 7H), 8.66 (s, 1H), 8.64 (d,  $J = 5.2$  Hz, 1H), 8.56 (s, 1H), 8.40 (s, 1H), 8.23–8.14 (m, 4H), 8.06 (d,  $J = 6.0$  Hz, 1H), 8.02–7.95 (m, 4H), 7.85 (d,  $J = 6.0$  Hz, 1H), 7.68 (m, 1H), 7.62–7.47 (m, 6H), 7.42 (m, 1H), 6.39 (s, 2H), 6.37 (s, 2H), 2.54 (s, 6H); ESI-MS:  $m/z$ : 613.143  $[\text{M} - 2\text{PF}_6]^{2+}$  (calcd for  $\text{C}_{54}\text{H}_{46}\text{N}_{10}\text{RuP}_2\text{F}_{12}$ : 613.112), 360.411  $[\text{M} - 3\text{PF}_6]^{3+}$  (calcd for  $\text{C}_{54}\text{H}_{46}\text{N}_{10}\text{RuP}_2\text{F}_{12}$ : 360.420); elemental analysis (%) calcd for  $\text{C}_{54}\text{H}_{46}\text{N}_{10}\text{RuP}_2\text{F}_{24} \cdot 2\text{H}_2\text{O}$  (1551.97): C 41.79, H 3.25, N 9.03; found: C 41.59, H 3.13, N 9.04.

All solvents for synthesis were used as received. All reactions and purifications were performed under dim light. Chromatographic purifications were carried out on Merck silica gel 60 (230–400 mesh), and thin-layer chromatography was performed on Merck silica gel 60  $\text{F}_{254}$ .

$^1\text{H}$  and  $^{13}\text{C}$  NMR spectra were recorded on Varian 300 MHz or on 400 MHz spectrometers. The electrospray ionization mass spectrometry (ESI-MS) experiments were carried out on a ZetSpec mass spectrometer (VG Analytical, Fisons Instrument) under the following conditions: needle potential, 3 kV; acceleration voltage, 4 kV; bath and nebulizing gas, nitrogen. Liquid flow was  $50 \mu\text{L min}^{-1}$  by using a syringe pump (Phoenix 20, Carlo Erba, Fisons instrument). The solvent used was acetonitrile (HPLC).

The amount of free  $[\text{Ru}(\text{bpy})_3]^{2+}$  impurity in  $[\text{Ru}(\text{bpy})_3-\text{MV}](\text{PF}_6)_4$  was determined to be less than 1% by comparing the magnitude of the steady-state emission to that of a  $[\text{Ru}(\text{bpy})_3](\text{PF}_6)_2$  standard with the same absorption at the excitation wavelength.

## Acknowledgement

This work was supported by the Swedish Foundation for Strategic Research (SSF), The Swedish Research Council for Engineering Sciences (TFR), and by the Wallenberg Foundation.

- [1] a) C. R. Bock, T. J. Meyer, D. G. Whitten, *J. Am. Chem. Soc.* **1974**, 96, 4710; b) K. Kalyanasundaram, *Photochemistry of Polypyridine and Porphyrin Complexes*, Academic Press, London, **1992**; c) N. Serpone in *Photoinduced Electron Transfer*, Vol. D (Eds.: M. A. Fox, M. Chanon), Elsevier, Amsterdam, **1988**, p. 47; d) K. Kalyanasundaram, *Chem. Phys. Lett.* **1982**, 88, 4; e) J. R. Darwent, K. Kalyanasundaram, *J. Chem. Soc. Faraday Trans. 2* **1981**, 77, 373.
- [2] a) C. L. Bird, A. T. Kuhn, *Chem. Soc. Rev.* **1981**, 10, 49; b) E. M. Kosower, J. L. Cotter, *J. Am. Chem. Soc.* **1964**, 86, 5524; c) P. M. S. Monk, *The Viologens*, Wiley, Chichester, **1998**.
- [3] See, for example, a) "Molecular Electronics: Science and Technology": *Ann. N.Y. Acad. Sci.* **1998**, 852, whole volume; b) V. Balzani, F. Scandola in *Comprehensive Supramolecular Chemistry*, Vol 10 (Eds.: J.-M. Lehn, J. L. Atwood, J. E. D. Davies, D. D. MacNicol, F. Vögtle, D. N. Reinhoudt), Pergamon, Oxford, **1996**; c) A. P. De Silva, H. Q. N. Gunaratne, T. Gunnlaugsson, A. J. M. Huxley, C. P. McCoy, J. T. Rademacher, T. E. Rice, *Chem. Rev.* **1997**, 97, 1515.
- [4] a) R. T. Hayes, M. R. Wasielewski, D. Gosztola, *J. Am. Chem. Soc.* **2000**, 122, 5563; b) A. S. Lukas, S. E. Miller, M. R. Wasielewski, *J. Phys. Chem. B* **2000**, 104, 931.
- [5] See refs. [1b, 2a, 7, 11].
- [6] a) E. H. Yonemoto, R. L. Riley, Y. I. Kim, S. J. Atherton, R. H. Schmehl, T. E. Mallouk, *J. Am. Chem. Soc.* **1992**, 114, 8081; b) E. H. Yonemoto, G. B. Saupe, R. H. Schmehl, S. M. Hubig, R. L. Riley, B. L. Iverson, T. E. Mallouk, *J. Am. Chem. Soc.* **1994**, 116, 4786.
- [7] T. Watanabe, K. Honda, *J. Phys. Chem.* **1982**, 86, 2617.
- [8] a) See ref. [2b]; b) D. Meisel, W. A. Mulac, M. S. Matheson, *J. Phys. Chem.* **1981**, 85, 179.
- [9] A. Yoshimura, M. Z. Hoffman, H. Sun, *Photochem. Photobiol. A* **1993**, 29.
- [10] The very narrow absorption band of  $\text{MV}^{++}$  around 400 nm appears to be less intense in the flash photolysis transient spectra relative to the spectra obtained by spectroelectrochemistry owing to the lower spectral resolution (10 nm bandpass) of the flash photolysis spectrometer.
- [11] A. Juris, V. Balzani, F. Barigelli, S. Campagna, P. Belser, A. von Zelewsky, *Coord. Chem. Rev.* **1988**, 84, 85.
- [12] a) T. Ohno, A. Yoshimura, D. R. Prasad, M. Z. Hoffman, *J. Phys. Chem.* **1991**, 95, 4723; b) C. D. Clark, M. Z. Hoffman, *J. Phys. Chem.* **1996**, 100, 7526.
- [13] N. J. Turro, *Modern Molecular Photochemistry*, Cummings, Menlo Park, **1978**.
- [14] a) J. Keizer, *Chem. Rev.* **1987**, 87, 167, and references therein; for recent studies of transient effects in bimolecular electron transfer, see b) A. D. Scully, S. Hirayama, K. Fukushima, T. Tominaga, *J. Phys. Chem.* **1993**, 97, 10524; c) S. Murata, M. Nishimura, S. Matsuzaki, M. Tachiya, *Chem. Phys. Lett.* **1994**, 219, 200.
- [15] R. A. Marcus, N. Sutin, *Biochim. Biophys. Acta* **1985**, 811, 265.
- [16] Note, however, that the electronic states of the reactant are different in the various reactions, so that a comparison based on differences only in driving force may not be entirely valid. In particular, reaction (1a) involves the oxidized  $[\text{Ru}(\text{bpy})_3]^{3+}$ , in which a vacancy is created in a metal-based orbital, while reactions (1b) and (1c) involve  $[\text{Ru}(\text{bpy})_3]^+$ , which has an excess electron on one bipyridine ligand. This may affect the electronic coupling differently, also in a bimolecular reaction.
- [17] See ref. [1d].
- [18] H. Sun, A. Yoshimura, M. Z. Hoffman, *J. Phys. Chem.* **1994**, 98, 5058.
- [19] L. A. Kelly, M. A. J. Rodgers, *J. Phys. Chem.* **1995**, 99, 13 132.
- [20] a) M. Tachiya, S. Murata, *J. Phys. Chem.* **1992**, 96, 8441; b) A. I. Buhrstein, E. Krissinel, *J. Phys. Chem.* **1996**, 100, 3005.
- [21] a) A. Ledwith, *Acc. Chem. Res.* **1972**, 5, 133; b) Ref. [1a].
- [22] a) T. Förster, *Ann. Phys.* **1948**, 2, 55; b) J. B. Birks, *Photophysics of Aromatic Molecules*, Wiley, London, **1970**, p. 569.
- [23] See refs. [1b, 11].
- [24] a) N. H. Damrauer, G. Cerullo, A. Yeh, T. R. Boussie, C. V. Shank, J. K. McCusker, *Science* **1997**, 275, 54; b) A. T. Yeh, C. V. Shank, J. K. McCusker, *Science* **2000**, 289, 935.
- [25] R. E. Hester, S. Susuki, *J. Phys. Chem.* **1982**, 86, 4626.
- [26] Y. Huang, J. B. Hopkins, *J. Phys. Chem.* **1996**, 100, 9585.
- [27] C. D. Clark, J. D. Debad, E. H. Yonemoto, T. E. Mallouk, A. J. Bard, *J. Am. Chem. Soc.* **1997**, 119, 10525.
- [28] A. J. Bard, L. R. Faulkner, *Electrochemical Methods*, Wiley, New York, **1980**.
- [29] With a reorganization energy of  $\lambda \approx 1.0$  eV, back reaction (2b) is activationless, while the activation energy ( $\Delta G^* = (\Delta G^0 + \lambda)^2/4\lambda$ ) for back reaction (2c) is ca. 27 meV, which would reduce the rate constant only by a factor of three.
- [30] a) Ref. [19]; b) L. F. Cooley, S. L. Larson, C. M. Elliot, D. F. Kelley, *J. Phys. Chem.* **1991**, 95, 10694.
- [31] L. F. Cooley, P. Bergquist, D. F. Kelley, *J. Am. Chem. Soc.* **1990**, 112, 2612.
- [32] M. Anderson, J. Davidson, L. Hammarström, J. Korppi-Tommola, T. Peltola, *J. Phys. Chem. B* **1999**, 103, 3258.
- [33] a) L. Sun, H. Berglund, R. Davydov, T. Norrby, L. Hammarström, P. R. Korall, A. Börje, C. Philouze, K. Berg, A. Tran, M. Andersson, G. Stenham, J. Mårtensson, M. Almgren, S. Styring, B. Åkermar, *J. Am. Chem. Soc.* **1997**, 119, 6996; b) O. Johansson, unpublished results.

Received: May 31, 2001 [F3305]